www.ietdl.org

Published in IET Biometrics
Received on 1st September 2013
Revised on 15th January 2014
Accepted on 10th February 2014
doi: 10.1049/iet-bmt.2013.0067

Special Issue: Integration of Biometrics and Forensics

ISSN 2047-4938

Regional fusion for high-resolution palmprint recognition using spectral minutiae representation

Ruifang Wang[1], Daniel Ramos[1], Raymond Veldhuis[2], Julian Fierrez[1], Luuk Spreeuwers[2], Haiyun Xu[3]

[1]*Biometric Recognition Group-ATVS, EPS, Universidad Autonoma de Madrid, Spain*
[2]*Signals and Systems Group, EEMCS, University of Twente, The Netherlands*
[3]*Software Improvement Group B.V., Amsterdam, The Netherlands*
E-mail: ruifang.wang@uam.es

Abstract: The spectral minutiae representation (SMC) has been recently proposed as a novel method to minutiae-based fingerprint recognition, which is invariant to minutiae translation and rotation and presents low computational complexity. As high-resolution palmprint recognition is also mainly based on minutiae sets, SMC has been applied to palmprints and used in full-to-full palmprint matching. However, the performance of that approach was still limited. As one of the main reasons for this is the much bigger size of a palmprint compared with a fingerprint, the authors propose a division of the palmprint into smaller regions. Then, to further improve the performance of spectral minutiae-based palmprint matching, in this work the authors present anatomically inspired regional fusion while using SMC for palmprints. Firstly, the authors consider three regions of the palm, namely interdigital, thenar and hypothenar, which have inspiration in anatomic cues. Then, the authors apply SMC to region-to-region palmprint comparison and study regional discriminability when using the method. After that, the authors implement regional fusion at score level by combining the scores of different regional comparisons in the palm with two fusion methods, that is, sum rule and logistic regression. The authors evaluate region-to-region comparison and regional fusion based on spectral minutiae matching on a public high-resolution palmprint database, THUPALMLAB. Both manual segmentation and automatic segmentation are performed to obtain the three palm regions for each palm. Essentially using the complex SMC, the authors obtain results on region-to-region comparison which show that the hypothenar and interdigital regions outperform the thenar region. More importantly, the authors achieve significant performance improvements by regional fusion using regions segmented both manually and automatically. One main advantage of the approach the authors took is that human examiners can segment the palm into the three regions without prior knowledge of the system, which makes the segmentation process easy to be incorporated in protocols such as in forensic science.

1 Introduction

Recently, the spectral minutiae representation (SMC) [1, 2] has shown its power in minutiae-based fingerprint recognition, which can handle minutiae translation and rotation with good computational efficiency at the matching stage, satisfying the requirements of high-resolution palmprint recognition as well. As defined in [1], the method uses the minutiae locations in spatial domain and takes Fourier transform of the coded locations and obtains the magnitude of its Fourier spectrum in frequency domain. The three types of SMCs are the location-based SMC (SML), the orientation-based SMC and the complex SMC, among which the enhanced SMC method [2] performs best for fingerprints with the EER of 3.05% on FVC2002 DB2A database [3] and a matching speed of 8000 comparisons per second. Inspired by matching accuracy and efficiency of SMC, we applied it to high-resolution palmprints captured at 500 ppi at least and implemented full-to-full palmprint comparison in a previous work [4], as high-resolution palmprint recognition is also mainly based on minutiae sets. However, the performance of SMC for full-to-full palmprint comparison is not satisfying compared with either its use in fingerprint matching or state-of-the-art in high-resolution palmprint recognition [5–8]. This is partly because of the big size of palmprints compared with fingerprints. This motivates us to improve the performance of spectral minutiae-based high-resolution palmprint recognition by using unique properties of high-resolution palmprint images.

Different from a fingerprint image, a high-resolution palmprint image, as shown in Fig. 1, is deemed to have rich types of features beyond minutiae, such as principal lines (major creases), and minor creases. Also, a palmprint can be divided into three regions by the three major creases, that is, interdigital, thenar and hypothenar, which is a typical division used in forensic anthropology for instance (see Fig. 1). As indicated in [9], the three palm regions divided by three major creases, have different performance according to matching accuracy, with the thenar region having much lower accuracy than interdigital and hypothenar regions. This property can be considered as a unique aspect of palmprints while it does not exist in fingerprints.

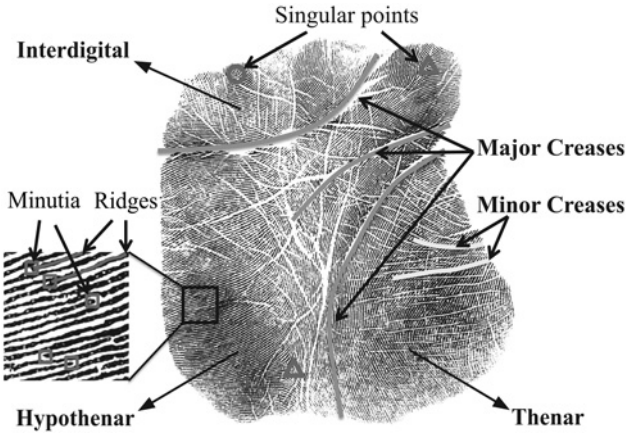

Fig. 1 *A sample full palmprint with high-resolution and its feature types*

Moreover, available high-resolution palmprint matching algorithms [5–7] essentially follow the minutiae-based fingerprint matching strategy and focus on full-to-full/partial-to-full palmprint comparison. These algorithms would face problems when they are applied to forensic palmprint recognition where latent marks have much smaller area than full palmprints, which was also argued in a recent work on forensic palmprint recognition [8]. This is an additional reason towards the division in regions of the palmprint in order to improve the performance of palmprint recognition in forensic applications.

Owing to the motivations described above, in this work, we present anatomically inspired regional fusion while using SMC for palmprints. Firstly, we apply SMC to region-to-region palmprint comparison and study discriminability in interdigital, thenar and hypothenar regions, respectively. Then, aimed to improve the performance, we implement regional fusion at score level and obtain results with two fusion methods, that is, sum rule [10, 11] and logistic regression [12, 13]. Both manual segmentation and automatic segmentation are performed to obtain the three palm regions for each palm. We evaluate region-to-region comparison and regional fusion based on spectral minutiae matching on a public high-resolution palmprint database, THUPALMLAB [14]. Essentially using the complex SMC, we obtain results on region-to-region comparison which show that the hypothenar and interdigital regions outperform the thenar region. More importantly, we achieve significant improvements by regional fusion using regions segmented both manually and automatically: (i) for manually segmented regions, EER of 3.64% for sum rule fusion, and 3.21% for logistic regression based fusion, showing an improvement of 10.56 and 10.99% in EER, respectively, compared with full-to-full palmprint comparison on the same testing dataset; and (ii) for automatically segmented regions, EER of 2.4% for sum rule fusion, and 1.77% for logistic regression based fusion, showing an improvement of 9.24% and 9.87% in EER, respectively, compared with full-to-full palmprint comparison on the same testing dataset.

This paper is an extension of the work on full-to-full palmprint comparison using SMC [4]. The major novelty is regional fusion using the three region-to-region palmprint comparison scores to significantly improve the performance of spectral minutiae matching for palmprints. The rest of the paper is organised as follows. Section 2 describes the SMC method. Section 3 shows an experimental study and analysis of regional discriminability while performing region-to-region palmprint comparison using SMC. Section 4 describes regional fusion based on sum rule and logistic regression, respectively, for high-resolution palmprint recognition and reports experimental results. Conclusions are given in Section 5.

2 Spectral minutiae representation

The SMC for high-resolution palmprints is the same as for fingerprints [1, 2]. Given the minutiae set $\{(x_i, y_i, \theta_i)\}_{i=1}^{Z}$ containing Z minutiae in a palmprint, the SMC consists of the following steps. Firstly, in spatial domain, the minutiae locations of a palmprint are coded by Gaussian indicator functions

$$m(x, y; \sigma^2) = \sum_{i=1}^{Z} \frac{1}{2\pi\sigma^2} \exp\left(-\frac{(x-x_i)^2 + (y-y_i)^2}{2\sigma^2}\right), \quad \sigma = \sigma_L \text{ or } \sigma_C \tag{1}$$

where $m(x, y; \sigma^2)$ is the summation of Gaussian indicator functions at the locations of all minutiae in a palmprint and σ is the standard deviation parameter. The parameters σ_L and σ_C denote the standard deviations for the SML representation and the SMC representation, respectively. Then, we take the Fourier transform of $m(x, y; \sigma^2)$ and obtain the magnitude of its Fourier spectrum, that is, for the SML representation [1]

$$\mathfrak{M}_L(\omega_x, \omega_y; \sigma_L^2) = \left|\exp\left(-\frac{\omega_x^2 + \omega_y^2}{2\sigma_L^{-2}}\right) \sum_{i=1}^{Z} \exp(-\mathrm{j}(\omega_x x_i + \omega_y y_i))\right| \tag{2}$$

and for the SMC representation [2],

$$\mathfrak{M}_C(\omega_x, \omega_y; \sigma_C^2) = \left|\exp\left(-\frac{\omega_x^2 + \omega_y^2}{2\sigma_C^{-2}}\right) \sum_{i=1}^{Z} \exp(-\mathrm{j}(\omega_x x_i + \omega_y y_i) + \mathrm{j}\theta_i)\right| \tag{3}$$

In the SML representation, only the location of a minutia is transformed, whereas both the location and orientation of a minutia are transformed in the SMC representation. Especially, when $\sigma = 0$, it means each minutia is presented by a Dirac pulse $m_i(x, y) = \delta(x - x_i, y - y_i)$, and the SML representation becomes

$$\mathfrak{M}_L(\omega_x, \omega_y; \sigma_L^2) = \sum_{i=1}^{Z} \exp(-\mathrm{j}(\omega_x x_i + \omega_y y_i)) \tag{4}$$

and the SMC representation becomes

$$\mathfrak{M}_C(\omega_x, \omega_y; \sigma_C^2) = \sum_{i=1}^{Z} \exp(-\mathrm{j}(\omega_x x_i + \omega_y y_i) + \mathrm{j}\theta_i) \tag{5}$$

Finally, the continuous spectra SML or SMC is sampled on a polar-linear grid with the size $M_0 \times N_0$ where M_0 (set to 128) samples are located in the radial direction between λ_l and λ_h, and N_0 (set to 256) samples are located in the angular

Table 1 Description of parameters for SMC and comparison

Parameters	Values	Descriptions
M	128	number of polar samples for radius
N	256	number of polar samples for angle
σ_L	≥ 0	Gaussian parameter for SML when 0, denotes dirac pulse; otherwise, Gaussian pulse
σ_C	≥ 0	Gaussian parameter for SMC when 0, denotes Dirac pulse; otherwise, Gaussian pulse
λ_l	≥ 0	lower bound of frequency range in the radial direction
λ_h	$> \lambda_l$	upper bound of frequency range in the radial direction
q	[−128, 128]	shift range setting for rotation compensation equivalent to a range [−180°, 180°] for SMC and a range [−90°, 90°] for SML

direction between 0 and π for SML or between 0 and 2π for SMC. Parameters λ_l and λ_h denote frequency range boundaries in the radial direction, which can be tuned during spectrum sampling.

Let R and T be the two sampled minutiae spectrums of dimensions $M \times N$ obtained from the minutiae sets in a reference palmprint and a test palmprint, respectively, the matching score between them is calculated as the maximum correlation coefficient between R and T as follows

$$S^{(R,T)} = \max_{p,q} \left| \frac{1}{MN} \sum_{m,n} R(m, n) T(m - p, n - q) \right|, \quad p = 0, q \in \left[-\frac{N}{2}, \frac{N}{2} \right] \tag{6}$$

where $T(m-p, n-q)$ denotes a shift version of $T(m, n)$ with a shift of p in the radial direction for scaling and a shift of q in the angular direction for rotation. In practice, we set $p = 0$ and assume that there is no scaling difference between the palmprints in the database we use since the database [14] is collected using a single palmprint scanner and the same protocol for all palmprints. Note that in this work we use the full angular shift range $[-N/2, N/2]$ in steps of one unit equivalent to a range [−180°, 180°] in steps of 1.4° for SMC and a range [−90°, 90°] in steps of 0.7° for SML for palmprint matching. This is because the palmprint images in the database we use have much larger rotation compared with previous works on fingerprints [1, 2] (e.g. in [1], a range [−15, 15] in steps of three units is used which is equivalent to a range [−10°, 10°] in steps of 2°). The parameters in (1)–(6) are summarised in Table 1. The above procedures of applying SMC to palmprints are similar with [4].

3 Region-to-region palmprint comparison

3.1 Regional discriminability

As observed from Figs. 1 and 2, the three palm regions have different feature properties: (i) the interdigital region contains significant singular points and the heart line which could improve its discriminability; (ii) the thenar region contains many more minor creases and wrinkles which deteriorate its discriminability; and (iii) the hypothenar region contains more regular ridges which improve its discriminability. To check these observations, we implemented region segmentation based on datum points [15] marked manually, and obtained region-to-region matching results using SMC on a subset of the database THUPALMLAB [14]. The subset of THUPALMLAB includes the palmprint images from the last 50 subjects with 100 palms, that is, 800 ($= 50 \times 2 \times 8$) images. Moreover, automatic segmentation based on datum points using the method proposed in [16] is also performed on the same subset. As reported in [16], there are 702 images segmented successfully in the subset of THUPALMLAB, among which there are 85 palms obtaining successful segmentation for their complete eight-image sets. We then use the 680 images from the 85palms and their automatically segmented regions to obtain region-to-region matching results.

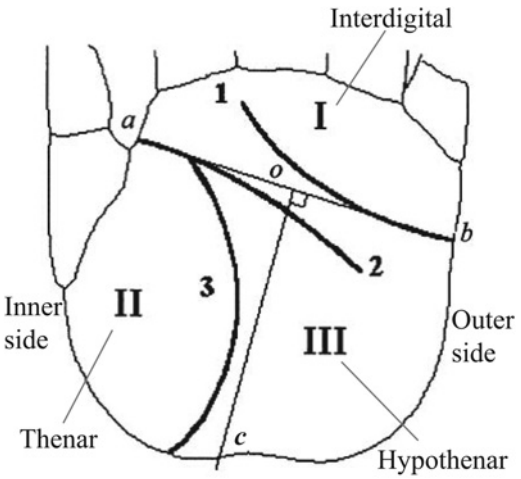

Fig. 2 *Definitions of a palmprint: principal lines (1 – heart line, 2 – head line and 3 – life line), palmprint regions (I – interdigital region, II – thenar region and III – hypothenar region) and datum points (a, b-endpoint, o-their midpoint) [15]. c is the intersection point of the bottom boundary of a palm and the perpendicular bisector of the line segment $\overline{ab}$. Here $\overline{ab}$ and $\overline{oc}$ are used for region segmentation.*

As both manual and automatic region segmentation techniques are inspired anatomically, here we first give a description of the anatomic basis of a palmprint. As shown in Fig. 2, because of the stability of the principal lines, the endpoints a and b of the life line and the heart line which intersect both sides of the palm, and their midpoint o are also stable according to their locations in the full palmprint. They were defined as datum points in [15]. Some significant properties of datum points can be used for region segmentation: (i) the relative locations of the endpoints and their midpoint are rotation invariant in a palmprint; and (ii) a palm can be divided into three regions: interdigital region (I), thenar region (II) and hypothenar region (III) by the connections between the endpoints and their perpendicular bisector, that is, line segments $\overline{ab}$ and $\overline{oc}$ (see Fig. 2).

Based on the properties of the datum points, we segment each palmprint into three regions manually and automatically, respectively. In the manual segmentation, we manually choose endpoints a and b according to their definition and obtain their position with X and Y axis values. In the automatic segmentation, endpoints a and b are detected automatically based on convex hull comparison as detailed in [16]. Then we calculate the position of their midpoint o. Finally we divide each palmprint into those

doi: 10.1049/iet-bmt.2013.0067

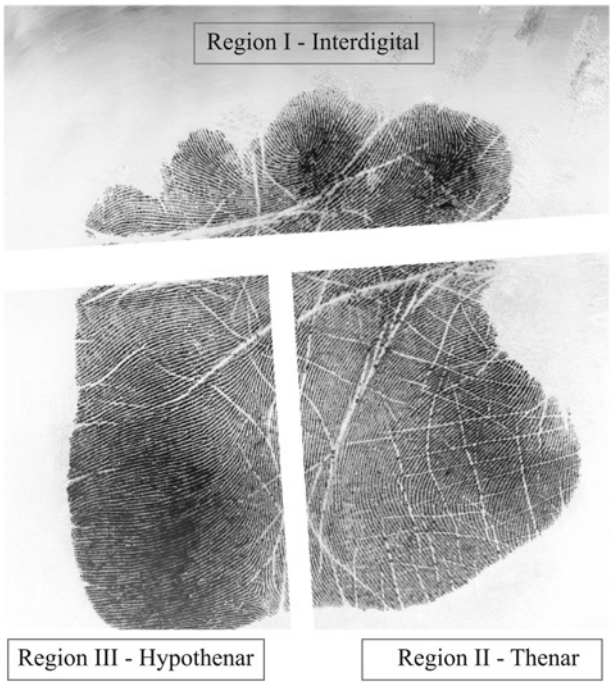

Fig. 3 *Segmented regions for a sample palmprint*

three regions by treating the line segments $\overline{ab}$ and $\overline{oc}$ as boundary lines. One example of manually segmented regions for a palmprint is shown in Fig. 3. Three regional datasets are generated from the testing database (800 palmprints) of THUPALMLAB after manual region segmentation and named as Region I, II and III corresponding to interdigital region (I), thenar region (II) and hypothenar region (III), respectively. And another three regional datasets are generated from the subset (680 palmprints) of the testing database after successful automatic region segmentation. These regional datasets will be used to obtain region-to-region matching scores in the next section.

3.2 Experimental analysis

In our experiments, we first use the commercial SDK MegaMatcher 4.0 [17] to implement feature extraction for the three regional datasets segmented manually and automatically, respectively, and then perform region-to-region comparison using SMC on the three regional datasets I, II and III separately.

For each regional dataset segmented manually, there are 2800 ($=(100\times8\times7)/2$) genuine comparison attempts and 4950 ($=(100\times99)/2$) impostor comparison attempts. Since the SMC method outperforms the SML method for palmprints as reported in [4], we only use the SMC method for region-to-region comparison. The best results with parameter configurations for the three regions are shown in Table 2, and the ROC curves are shown in Fig. 4. The EER results are 11.11, 17.5 and 5.46% corresponding to interdigital region, thenar region and hypothenar region, respectively. As it can be observed, the thenar region shows much lower discriminating power. This is consistent with the observation that the thenar region contains many more minor creases and wrinkles which deteriorate its discriminability. It is also consistent with the result reported in [9] when the matching is based on minutiae features. The results also show that the hypothenar region outperforms

Table 2 Results of region-to-region matching compared with full-to-full matching using the SMC method with Dirac pulse ($\sigma=0$)

Comparisons	Parameters $[\lambda_l, \lambda_h]$	EER	
		Manual regions, %	Automatic regions, %
interdigital (I)	[0.02, 0.3]	11.11	8.95
thenar (II)	[0.08, 0.25]	17.5	16.43
hypothenar (III)	[0.02, 0.16]	5.46	4.08
full-to-full	[0.06, 0.16]	14.2	11.64

the interdigital region on the THUPALMLAB database, which is possibly because that the hypothenar region has more minutiae with better quality owing to much less minor creases in this region than in the interdigital region. Furthermore, the interdigital and hypothenar regions outperform full-to-full comparison with EER of 14.2% using the SMC method, but not the thenar region. This evidences that not all the regions should receive equal treatment, like it happens in full-to-full comparison. This observation reinforces the motivation of regional fusion. Note that the selection of the parameters λ_l and λ_h is performed with several trials on the same testing database without using another training database. This is owing to that the aim of this work is to show how regional fusion can overcome the limitations of the SMC method, not the tuning of the method.

For each regional dataset segmented automatically, there are 2380 ($=(85\times8\times7)/2$) genuine comparison attempts and 3570 ($=(85\times84)/2$) impostor comparison attempts. The same parameter configurations as for the regional datasets segmented manually are used. The results are shown in Table 2, and the ROC curves are shown in Fig. 5. The EER results are 8.95, 16.43 and 4.08% corresponding to interdigital region, thenar region and hypothenar region, respectively. It also indicates that on the THUPALMLAB database, the thenar region shows much lower matching accuracy, which is consistent with the observation at the beginning of this section and the result reported in [9]. Moreover, the hypothenar region outperforms interdigital

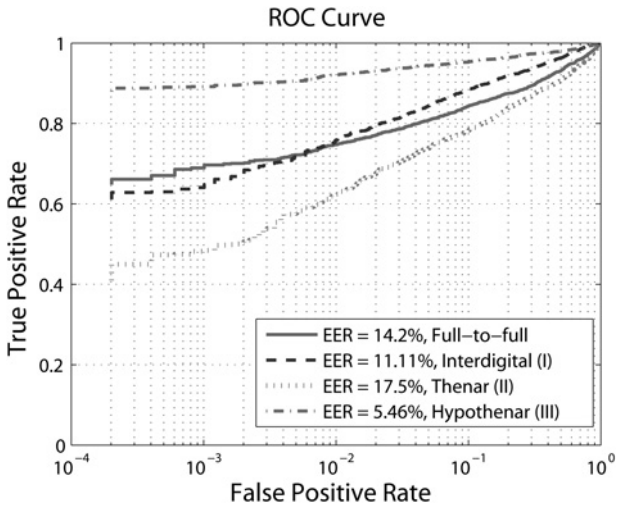

Fig. 4 *ROC curves for the three region-to-region comparisons using manually segmented regions compared with full-to-full matching on the subset of 800 palmprints from THUPALMLAB*

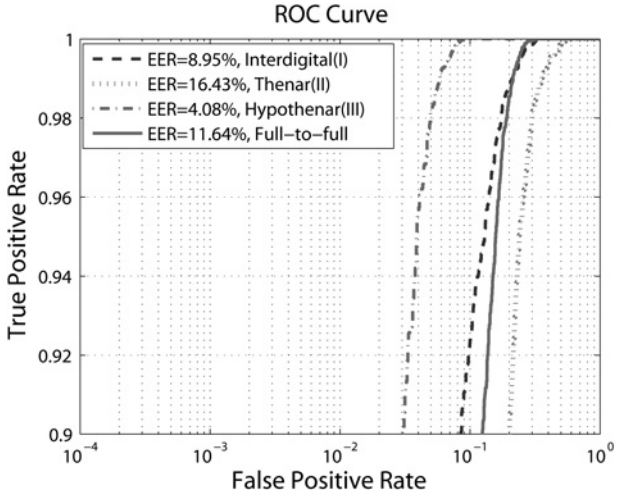

Fig. 5 *ROC curves for the three region-to-region comparisons using automatically segmented regions compared with full-to-full matching on the subset of 680 palmprints from THUPALMLAB*

region on the THUPALMLAB database, and also outperforms full-to-full comparison with EER of 11.64% using automatically segmented regions (note that the difference in EER between full-to-full comparison with manual and automatic segmentation is because of the slight difference between experimental datasets). It can be seen that the results are consistent with the performance on the regional datasets segmented manually, reinforcing the conclusions about regional discriminability. Again, the evidence that the different regions should receive different treatment is confirmed, and the motivation of regional fusion is supported.

4 Regional fusion

Based on the above experimental study on regional discriminability, we implement regional fusion for high-resolution palmprint recognition in this section, using regions segmented manually and automatically, respectively. As shown in Fig. 6, using region-to-region comparison scores obtained in Section 3, we obtain regional fused scores using two fusion methods, that is, sum rule

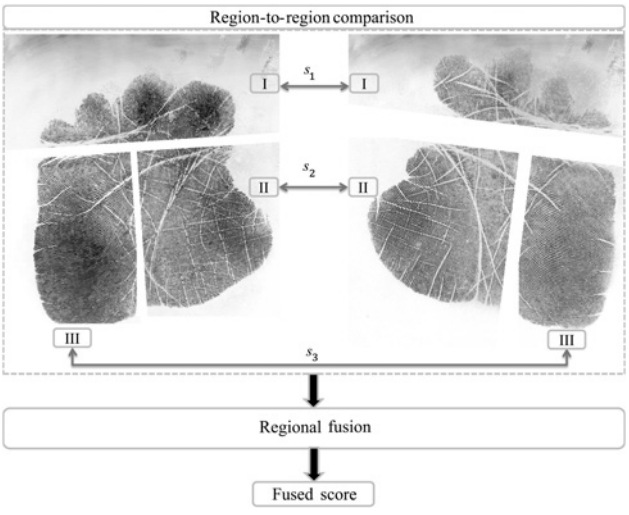

Fig. 6 *Matching strategy of regional fusion*

[10] and logistic regression [12, 13]. The implementation is detailed in the following sections.

4.1 Sum rule against logistic regression

Both fusion methods considered are using a linear combination of the score sets s_1, s_2, s_3 obtained from region-to-region comparison of the three regions. The sum rule fusion is simply represented as

$$s_{f1} = \sum_{i=1}^{3} s_i \tag{7}$$

and the logistic regression based score fusion is represented as

$$s_{f2} = w_0 + \sum_{i=1}^{3} w_i \cdot s_i \tag{8}$$

where s_{f1} and s_{f2} are the fused output scores, and $\boldsymbol{w} = [w_0, w_1, w_2, w_3]$ is a vector of real-valued weights trained using logistic regression (details given below).

4.2 Experimental analysis

In this section, we obtain regional fusion results using the two fusion methods described above, for regions segmented manually and automatically, respectively. The FoCal Toolkit [18] is used to implement logistic regression based score fusion. The testing databases from THUPALMLAB are the same as described in Section 3.2. Following a leave-one-out training scheme, that is, leaving out all the genuine and impostor scores corresponding to one palm in each iteration, we use both genuine and impostor training scores to estimate $\boldsymbol{w}$ using FoCal which implements maximum-likelihood training. This leave-one-out training scheme may lead to somewhat optimistic results, because the training and testing score sets are in comparable conditions in each iteration. However, as we will see, it performs in a comparable way as sum fusion which does

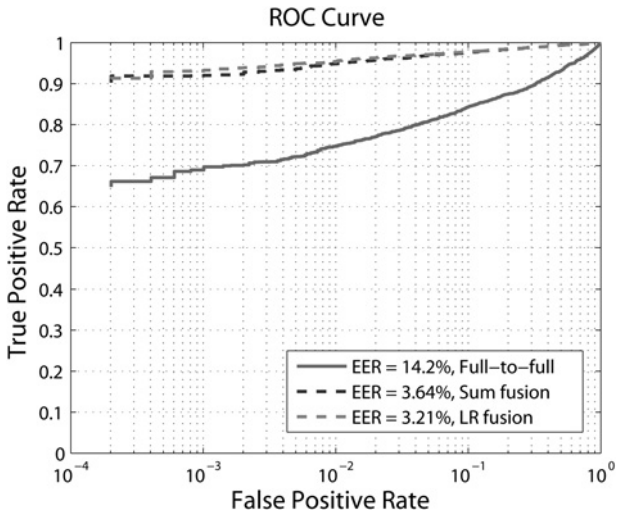

Fig. 7 *ROC curves of regional fusion based on sum rule and logistic regression, respectively, using manually segmented regions, compared with full-to-full comparison on the subset of 800 palmprints from THUPALMLAB*

doi: 10.1049/iet-bmt.2013.0067

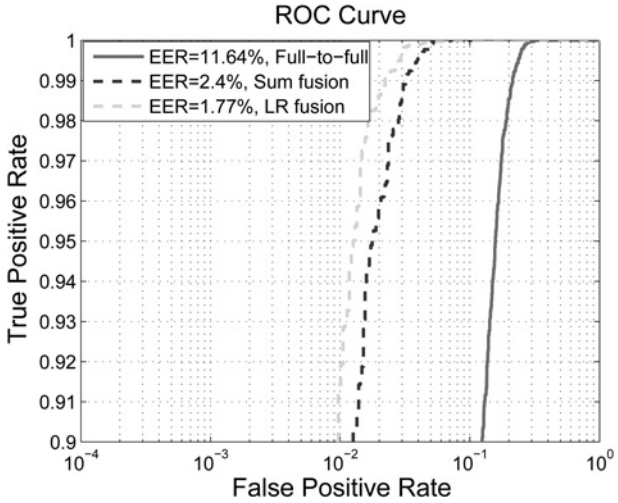

Fig. 8 *ROC curves of regional fusion based on sum rule and logistic regression, respectively, using automatically segmented regions, compared with full-to-full comparison on the subset of 680 palmprints from THUPALMLAB*

not require training. The latter diminishes the risk of overfitting.

The ROC curves of the two fusion methods on the regional datasets segmented manually are shown in Fig. 7. EER of 3.64% is achieved by sum fusion, whereas EER of 3.21% by logistic regression based score fusion. The results prove a significant improvement by regional fusion, compared with the EER results of 14.2% for full-to-full comparison and 11.11, 17.5 and 5.46% corresponding to the three individual region-to-region comparisons as reported in Section 3.2 for manual segmentation.

The ROC curves of the two fusion methods on the regional datasets segmented automatically are shown in Fig. 8. It can be seen that the ROC curves are also improved by regional fusion based on logistic regression and sum rule compared with full-to-full comparison. The EERs of regional fusion using logistic regression and sum rule are 2.4 and 1.77%, respectively, compared with 11.46% of full-to-full comparison and 8.95, 16.43 and 4.08% corresponding to the three individual region-to-region comparisons as reported in Section 3.2 for automatic segmentation. This also indicates that regional fusion outperforms region-to-region comparison as well as full-to-full comparison. Therefore the hypotheses which motivated this fusion method are confirmed.

5 Conclusions

In this work, we presented anatomically inspired regional fusion while using SMC for palmprints. Firstly, we applied SMC to region-to-region palmprint comparison and studied regional discriminability when using the SMC method in the three different regions of the palmprint, that is, interdigital, thenar and hypothenar. Evaluated on a subset of 680 palmprints from the public high-resolution palmprint database THUPALMLAB, the best EER results using regions segmented automatically were 8.95% for the interdigital region, 16.43% for the thenar region and 4.08% for the hypothenar region. Then, aimed to improve the performance further, we implemented regional fusion at score level using region-to-region comparison score sets and obtained results with two fusion methods, that is, sum rule and logistic regression. Using regions segmented automatically, The EER results of 2.4% for sum rule fusion, and 1.77% for logistic regression based fusion were achieved on the subset of 680 palmprints from THUPALMLAB. The results show that: (i) The hypothenar and interdigital regions outperform the thenar region; and (ii) regional fusion using both fusion methods significantly improves the performance of spectral minutiae matching for palmprints. Moreover, using regions segmented manually, similar conclusions were confirmed.

Worth noting, the contribution of this work is mainly based on regional fusion. Although the SMC method has severe limitations when applied to palmprints, regional fusion can still improve its performance. We can foresee other systems may also be able to achieve better performance by using regional fusion, which are to be tested. Regional fusion employs regional discriminability, which could be further applied to forensic applications, mainly latent-to-full palmprint comparison. Towards that direction, our future work will be: (i) improving automatic and database-adaptable region segmentation techniques under the concept of three regions; and (ii) applying region fusion based on automatic region segmentation to forensic palmprint comparison.

6 Acknowledgments

R. Wang is supported by the Marie Curie Fellowship under a EC project BBfor2 (FP7-ITN-238803). This work has also been partially supported by Spanish Guardia Civil, 'Cátedra UAM-Telefónica' and projects Bio-Shield (TEC2012-34881) and Contexts (S2009/TIC-1485).

7 References

1 Xu, H., Veldhuis, R., Bazen, A., Kevenaar, T., Akkermans, T., Gokberk, B.: 'Fingerprint verification using spectral minutiae representations', *IEEE Trans. Inf. Forensics Sec.*, 2009, **4**, (3), pp. 397–409
2 Xu, H., Veldhuis, R.N.: 'Complex spectral minutiae representation for fingerprint recognition'. Proc. IEEE Computer Society Conf. on Computer Vision and Pattern Recognition Workshops (CVPRW), San Francisco, USA, June 2010, pp. 1–8
3 University of Bologna: 'Fvc2002 fingerprint database'. Available: http://bias.csr.unibo.it/fvc2002/databases.asp, 2011
4 Wang, R., Veldhuis, R.N., Ramos, D., Spreeuwers, L., Fierrez, J., Xu, H.: 'On the use of spectral minutiae in high-resolution palmprint recognition'. Proc. Int. Workshop on Biometrics and Forensics (IWBF), Lisbon, Portugal, April 2013
5 Dai, J., Zhou, J.: 'Multifeature-based high-resolution palmprint recognition', *IEEE Trans. Pattern Anal. Mach. Intell.*, 2011, **33**, (5), pp. 945–957
6 Dai, J., Feng, J., Zhou, J.: 'Robust and efficient ridge-based palmprint matching', *IEEE Trans. Pattern Anal. Mach. Intell.*, 2012, **34**, (8), pp. 1618–1632
7 Cappelli, R., Ferrara, M., Maio, D.: 'A fast and accurate palmprint recognition system based on minutiae', *IEEE Trans. Syst., Man, Cybern. B*, 2012, **42**, (3), pp. 956–962
8 Liu, E., Jain, A., Tian, J.: 'A coarse to fine minutiae-based latent palmprint matching', *IEEE Trans. Pattern Anal. Mach. Intell.*, 2013, **35**, (10), pp. 2307–2322
9 Jain, A., Feng, J.: 'Latent palmprint matching', *IEEE Trans. Pattern Anal. Mach. Intell.*, 2009, **31**, (6), pp. 1032–1047
10 Kittler, J., Hatef, M., Duin, R.P., Matas, J.: 'On combining classifiers', *IEEE Trans. Pattern Anal. Mach. Intell.*, 1998, **20**, (3), pp. 226–239
11 'Score level fusion', in Ross, A.A., Nandakumar, K., Jain, A.K. (Eds.): 'Handbook of Multibiometrics' (Springer, New York, USA, 2006), ch. 4, pp. 91–142
12 Pigeon, S., Druyts, P., Verlinde, P.: 'Applying logistic regression to the fusion of the nist99 1-speaker submissions', *Digit. Signal Process.*, 2000, **10**, (1–3), pp. 237–248
13 Brummer, N., Burget, L., Cernocky, J., *et al.*: 'Fusion of heterogeneous speaker recognition systems in the stbu submission for the nist speaker

recognition evaluation 2006', *IEEE Trans. Audio Speech Lang. Process.*, 2007, **15**, (7), pp. 2072–2084
14 Tsinghua University: 'Thupalmlab palmprint database'. Available: http://ivg.au.tsinghua.edu.cn/index.php?n=Data. Tsinghua500ppi, 2011
15 Zhang, D., Shu, W.: 'Two novel characteristics in palmprint verification: datum point invariance and line feature matching', *Pattern Recognit.*, 1999, **32**, (4), pp. 691–702
16 Wang, R., Ramos, D., Fierrez, J., Krish, R.P.: 'Automatic region segmentation for high-resolution palmprint recognition: Towards forensic scenarios'. Proc. 47th Int. Carnahan Conf. on Security Technology (ICCST), Medellín, Colombia, October 2013
17 Neurotechnology: 'Megamatcher 4.0 sdk'. Available: http://www.neurotechnology.com, 2011
18 Brummer, N.: 'Focal toolkit'. Available: https: //sites.google.com/site/nikobrummer/focal, 2007

doi: 10.1049/iet-bmt.2013.0067